JOC Article

Phenothiazine Cruciforms: Synthesis and Metallochromic Properties

Martina Hauck,[†] Jan Schönhaber,[‡] Anthony J. Zucchero,[‡] Kenneth I. Hardcastle,[§] Thomas J. J. Müller,*[,†] and Uwe H. F. Bunz*[,‡]

School of Chemistry and Biochemistry, Georgia Institute of Technology, 901 Atlantic Drive, Atlanta, Georgia 30332, Department of Chemistry, Emory University, 1515 Dickey Drive, Atlanta, Georgia 30322-2210, and Institut für Organische Chemie und Makromolekulare Chemie, Heinrich-Heine-Universität, Universitätsstrasse 1, Gebäude 26.43.00.41, D-40225 Düsseldorf, Germany

uwe.bunz@chemistry.gatech.edu

Received May 3, 2007

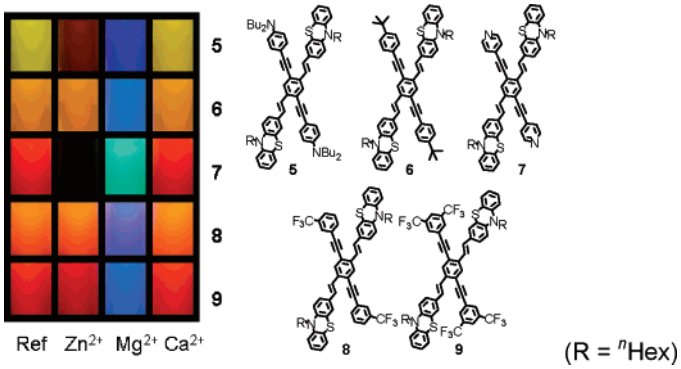

We report the synthesis and characterization of five novel phenothiazine-containing cruciforms (**5**−**9**). The targets were prepared by a NaH-promoted Horner reaction of tetraethyl(2,5-diiodo-1,4-phenylene)-bis(methylene)diphosphonate with 10-hexyl-10*H*-phenothiazine-3-carbaldehyde. The formed intermediary 3,3′-(1*E*,1′*E*)-2,2′-(2,5-diiodo-1,4-phenylene)bis(ethene-2,1-diyl)bis(10-hexyl-10*H*-phenothiazine) was reacted with several different aromatic alkynes (1-*tert*-butyl-4-ethynylbenzene, *N*,*N*-dibutyl-4-ethynylaniline, 1-ethynyl-3-(trifluoromethyl)benzene, and 1-ethynyl-3,5-bis(trifluoromethyl)benzene) to give the corresponding cruciform fluororphores (XF). The XFs were fully characterized by NMR and IR spectroscopy and then exposed to trifluoroacetic acid as well as to several metal triflates. The XFs show dramatic shifts in emission and to a lesser extent in absorption when exposed to magnesium triflate or zinc triflate. In the case of magnesium triflate, a blue shift in emission was observed; in contrast, addition of zinc triflate results in either quenching or a red-shifted emission. Due to the electronic situation, these XFs display spatially separated frontier molecular orbitals, allowing the HOMO or the LUMO of the XFs to be addressed independently by addition of zinc or magnesium ions. Phenothiazine XFs may have potential in array-type sensory applications for metal cations.

Introduction

Cruciform fluorophores (XFs) display two distinct molecular axes with either similar or dissimilar electronic properties. Examples of XFs are Haley's 1,2,4,5-tetraethynylbenzenes, Marks' X-shaped 1,2,4,5-tetravinylbenzene phores, and the distinct 1,4-bis(arylethynyl)-2,5-distyrylbenzenes.[1−3] Other cross-shaped fluorophores have been developed by Nuckolls and by Scherf.[4−7] Depending upon the employed molecular design, XFs have found applications as electroactive organic glasses in thin-

[†] Heinrich-Heine-Universität.
[‡] Georgia Institute of Technology.
[§] Emory University.

(1) (a) Samori, S.; Tojo, S.; Fujitsuka, M.; Spitler, E. L.; Haley, M. M.; Majima, T. *J. Org. Chem.* **2007**, *72*, 2785−2793. (b) Spitler, E. L.; Shirtcliff, L. D.; Haley, M. M. *J. Org. Chem.* **2007**, *72*, 86−96. (c) Marsden, J. A.; Miller, J. J.; Shirtcliff, L. D.; Haley, M. M. *J. Am. Chem. Soc.* **2005**, *127*, 2464−2476. (d) Slepkov, A. D.; Hegmann, F. A.; Tykwinski, R. R.; Kamada, K.; Ohta, K.; Marsden, J. A.; Spitler, E. L.; Miller, J. J.; Hayley, M. M. *Opt. Lett.* **2006**, *31*, 3315−3317.

10.1021/jo070922l CCC: $37.00
Published on Web 08/10/2007

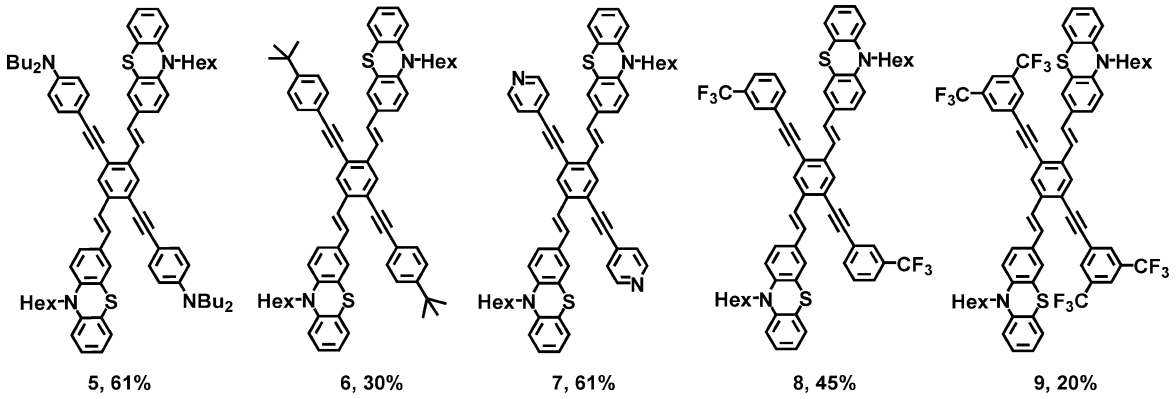

FIGURE 1. Synthesized phenothiazine-substituted cruciforms.

SCHEME 1. Synthesis of Phenothiazine-Containing Cruciforms

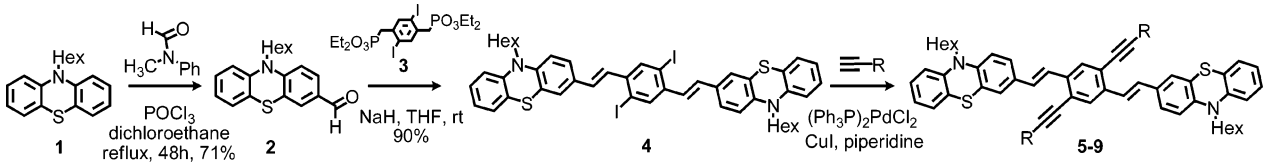

film transistors, organic single-layer device components, nonlinear optical materials, and most notably as responsive fluorophore cores.[1−5] Responsive XF cores with 1,2,4,5-tetra-substituted benzenes display two transverse π-systems connected by a central benzene ring (Figure 1). This specific structure leads to large metallochromic and acidochromic shifts in absorption and emission, significantly larger than those recorded for similar distyrylbenzene derivatives lacking the second transverse.[8] The increased response of XFs toward external stimuli such as protons or metal cations is a consequence of their unusual frontier orbital structure.[3] If one transverse of an XF is doubly acceptor substituted and the other doubly donor substituted, HOMO and LUMO become localized on the donor and acceptor branches, respectively. As a consequence of this orbital arrangement, binding of a positively charged species to the donor branch will affect the HOMO and lower its energy but will leave the LUMO unchanged, resulting in a blue-shifted absorption and emission. If a positively charged species is bound to the acceptor branch, the opposite occurs; the LUMO is stabilized and the HOMO−LUMO gap shrinks. This unique FMO arrangement permits one to independently address either HOMO or LUMO. Up to now, XFs exclusively contained pyridine and/or dialkylamino groups as metal binding sites.[1,3] In this contribution, we describe the synthesis, characterization, and metallochromic properties of phenothiazine-substituted XFs.[1,3] Phenothiazines are easily and reversibly oxidized as electron-rich tricyclic heterocycles.[9] As strong electron donors, they have found application in electroactive materials with donor−acceptor character.[10] Phenothiazine-containing systems show promise for the synthesis of metallochromic XFs.

Results and Discussion

Synthesis. Starting from 10-hexyl-10*H*-phenothiazine, Vilsmeier formylation of **1** with phosphorus oxychloride and *N*-methylformanilide in 1,2-dichloroethane regioselectively furnishes the aldehyde **2** in 71% yield as bright yellow crystals.[9d,10]

(2) (a) Kang, H.; Evmenenko, G.; Dutta, P.; Clays, K.; Song, K.; Marks, T. J. *J. Am. Chem. Soc.* **2006**, *128*, 6194−6205. (b) Hu, K.; Zhu, P. W.; Yu, Y.; Facchetti, A.; Marks, T. J. *J. Am. Chem. Soc.* **2004**, *126*, 15974−15975.

(3) (a) Wilson, J. N.; Bunz, U. H. F. *J. Am. Chem. Soc.* **2005**, *127*, 4124−4125. (b) Wilson, J. N.; Josowicz, M.; Wang, Y. Q.; Bunz, U. H. F. *Chem. Commun.* **2003**, 2962−2963. (c) Zucchero, A. J.; Wilson, J. N.; Bunz, U. H. F. *J. Am. Chem. Soc.* **2006**, *128*, 11872−11881. (d) Gerhardt, W. W.; Zucchero, A. J.; Wilson, J. N.; South, C. R.; Bunz, U. H. F.; Weck, M. *Chem. Commun.* **2006**, 2141−2142.

(4) (a) Miao, Q.; Chi, X. L.; Xiao, S. X.; Zeis, R.; Lefenfeld, M.; Siegrist, T.; Steigerwald, M. L.; Nuckolls, C. *J. Am. Chem. Soc.* **2006**, *128*, 1340−1345. (b) Klare, J. E.; Tulevski, G. S.; Sugo, K. de Picciotto, A.; White, K. A.; Nuckolls, C. *J. Am. Chem. Soc.* **2003**, *125*, 6030−6031.

(5) (a) Zen, A.; Bilge, A.; Galbrecht, F.; Alle, R.; Meerholz, K.; Grenzer, J.; Neher, D.; Scherf, U.; Farrell, T. *J. Am. Chem. Soc.* **2006**, *128*, 3914−3915. (b) Thompson, A. L.; Ahn, T. S.; Thomas, K. R. J.; Thayumanavan, S.; Martinez, T. J.; Bardeen, C. J. *J. Am. Chem. Soc.* **2005**, *125*, 16348−16349. (c) Meier, H.; Mühling, B.; Kolshorn, H. *Eur. J. Org. Chem.* **2004**, 1033−1042. (d) Gerhardt, W. W.; Zucchero, A. J.; South, C. R.; Bunz, U. H. F.; Weck, M. *Chem. Eur. J.* **2007**, *13*, 4467−4474. (e) McGrier, P. L.; Solntsev, K. M.; Schönhaber, J.; Brombosz, S. M.; Tolbert, L. M.; Bunz, U. H. F. *Chem. Commun.* **2007**, 2127−2129.

(6) Wang, S. J.; Oldham, W. J.; Hudack, R. A.; Bazan, G. C. *J. Am. Chem. Soc.* **2000**, *122*, 5695−5709.

(7) (a) Tolosa, J.; Diez-Barra, E.; Sanchez-Verdu, P.; Rodriguez-Lopez, J. *Tetrahedron Lett.* **2006**, *47*, 4647−4651. (b) Niazimbetova, Z. I.; Christian, H. Y.; Bhandari, Y. J.; Beyer, F. L.; Galvin, M. E. *J. Phys. Chem. B* **2004**, *108*, 8673−8681. (c) Sorensen, J. K.; Vestergaard, M.; Kadziola, A.; Kilsa, K.; Nielsen, M. B. *Org. Lett.* **2006**, *8*, 1173−1176.

(8) (a) Detert, H.; Schmitt, V. *J. Phys. Org. Chem.* **2006**, *19*, 603−607. (b) Detert, H.; Sugiono, E. *J. Lumin.* **2005**, *112*, 372−376. (c) Detert, H.; Stalmach, U.; Sugiono, E. *Synth. Met.* **2004**, *147*, 227−231. (d) Detert, H.; Sadovshi, L.; Sugiono, E. *J. Phys. Org. Chem.* **2004**, *17*, 1046−1050. (e) Meier, H.; Mühling, B.; Kolshorn, H. *Eur. J. Org. Chem.* **2004**, 1033−1024.

(9) (a) Sainsbury, M. In *Rodd's Chemistry of Carbon Compounds* 2nd ed.; Sainsbury, M., Ed.; Elsevier: Amsterdam, 1998; Vol. 4, pp 575−608. (b) Sainsbury, M. In *Comprehensive Heterocyclic Chemistry*; Katritzky, A. R., Rees, C. W., Eds.; Pergamon Press: Oxford, New York, Toronto, Sydney, Paris, Frankfurt, 1984; Vol. 3, p 995. (c) McIntyre, R.; Gerischer, H. *Ber. Bunsen-Ges. Phys. Chem.* **1984**, *88*, 963−969. (d) Krishna, R. M.; Kurshev, V.; Kervan, L. *Phys. Chem. Chem. Phys.* **1999**, *11*, 2833−2840.

(10) (a) Bucci, N.; Müller, T. J. J. *Tetrahedron Lett.* **2006**, *47*, 8329−8332. (b) Bucci, N.; Müller, T. J. J. *Tetrahedron Lett.* **2006**, *47*, 8323−8327. (c) Sailer, M.; Nonnenmacher, M.; Oeser, T.; Müller, T. J. J. *Eur. J. Org. Chem.* **2006**, 423−435. (d) Kramer, C. S.; Müller, T. J. J. *Eur. J. Org. Chem.* **2003**, 3534−3548.

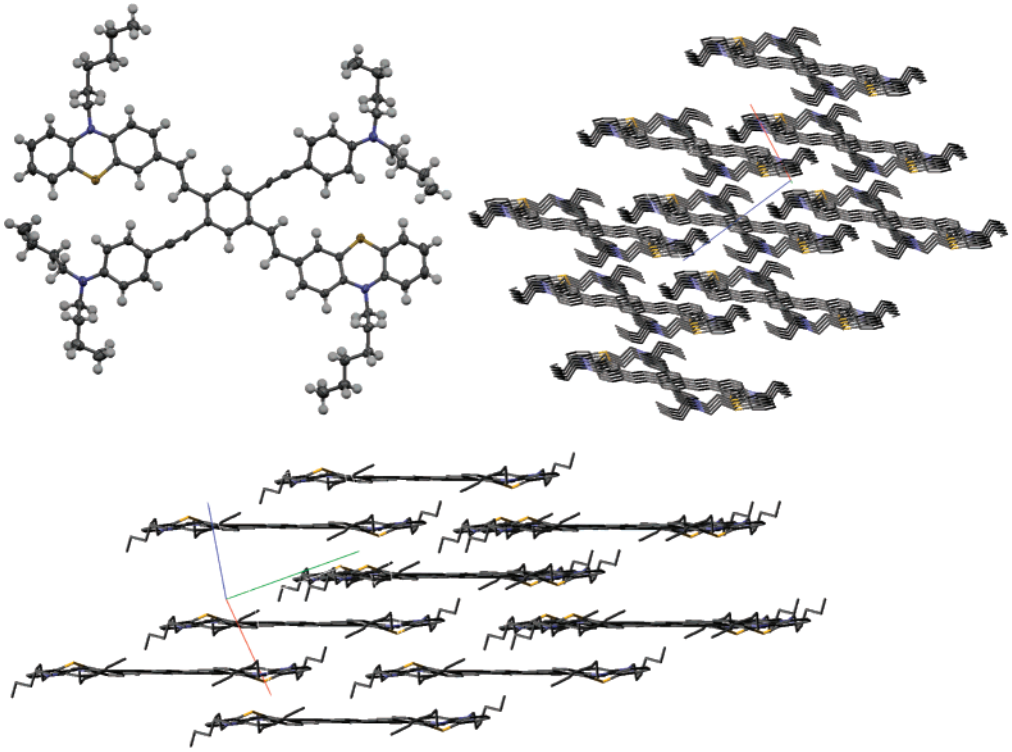

FIGURE 2. Molecular structure of **5** (top left). Packing of **5** seen along the *b*-axis. Blue: *c*-axis, green: *b*-axis, red: *a*-axis (top right). View of the packing of **5** along the planar π-system (bottom).[13]

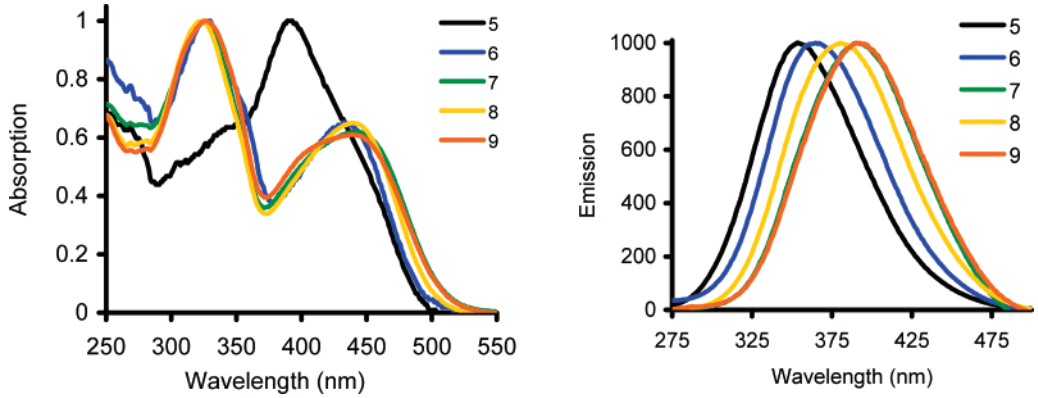

FIGURE 3. Absorption (left) and emission (right) spectra of the cruciforms **5**−**9** in dichloromethane.

TABLE 1. Spectroscopic and Quantum Chemical Data for the Cruciforms 5−9 in Dichloromethane

	5	6	7	8	9
λ_{max} abs (nm)	392	433	442	437	439
λ_{max} abs (nm) +H^+	→[a] 432 (40 equiv) → 332 (1000 equiv)	→ 331 (800 equiv)	→ 422 (2.0 equiv) → 349 (1400 equiv)	na	na
λ_{max} emission (nm)	552	563	589	579	590
λ_{max} emission (nm) +H^+	→ 577 (40 equiv) → 417 (1000 equiv)	→ 447 (800 equiv)	→ q[b] (2.0 equiv) → 528 (1400 equiv)	na	na
Stokes shift (cm^{-1})	7717	5528	5637	5619	6566
Φ	0.53	0.36	0.07	0.25	0.16
HO, LU calcd (eV)	(**5′**) −4.46, −1.62	(**6′**) −4.74, −1.95	(**7′**) −4.91, −2.32	na	na
band gap calcd (eV)	(**5′**) 2.84	(**6′**) 2.79	(**7′**) 2.59		

[a] Arrow (→) depicts addition of increasing amounts of acid. [b] q: fluorescence is quenched.

A subsequent Horner reaction of the diphosphonate **3** with the phenothiazine aldehyde **2** afforded **4** in 90% yield after recrystallization.[10,11] Palladium-catalyzed coupling of the diiodide **4** to different alkynes accessed the phenothiazine-based XFs **5**−**9** in 20−61% yield (Scheme 1). The XFs were obtained as yellow-to-red colored crystalline powders that were identified

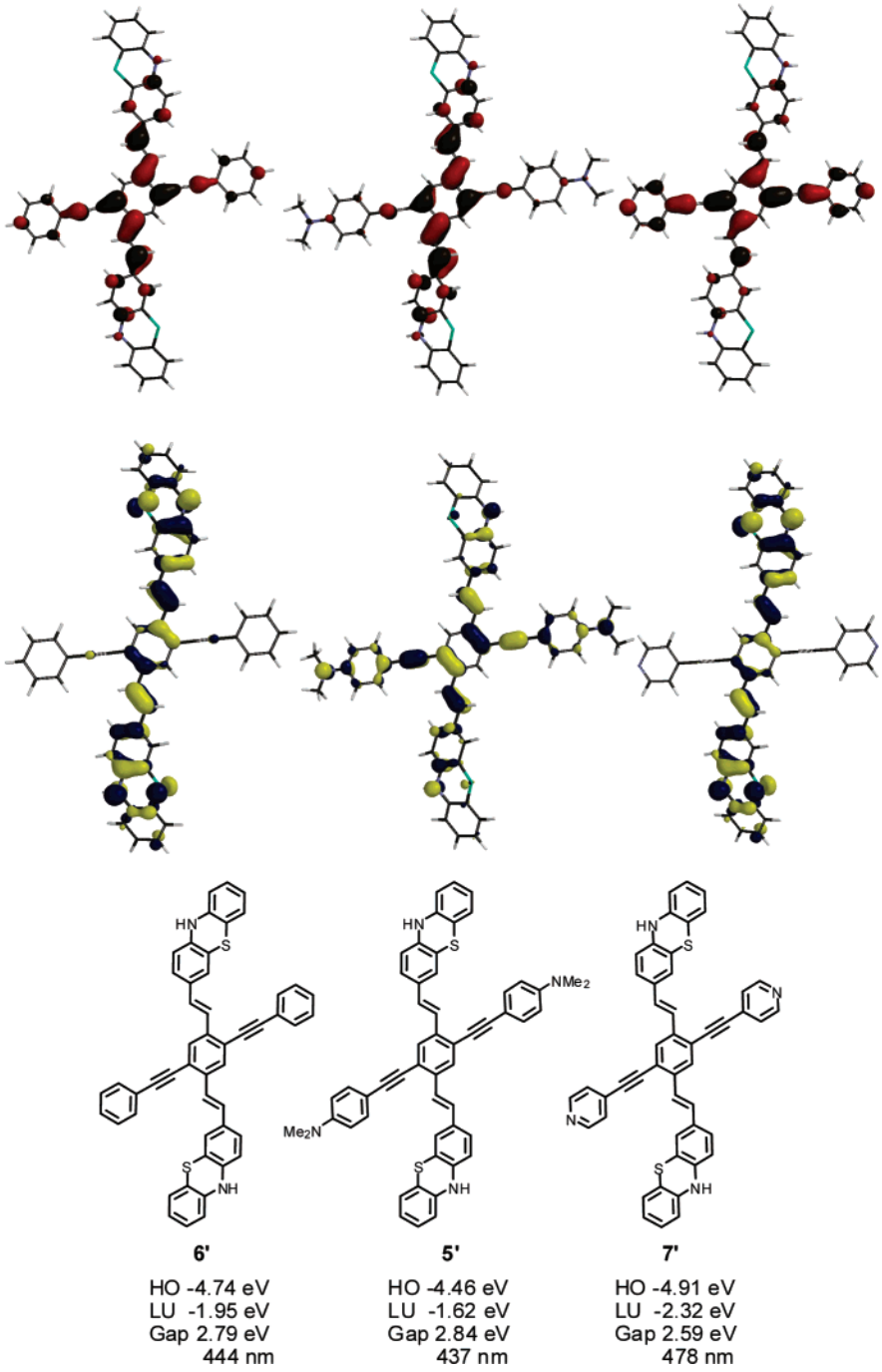

FIGURE 4. Molecular orbital plots (LUMOs, top; HOMOs, bottom) of cruciforms **5′**−**7′**. The calculations were performed using B3LYP/6-31G*//6-31G* as implemented on SPARTAN.

by their characteristic ^{1}H and ^{13}C NMR signals. To fully corroborate the presence of the XF core, we obtained diffraction quality specimens of XF **5**. Figure 2 shows the structure and the packing of XF **5** in the solid state. The bond lengths and bond angles are in excellent agreement with expected values and are very similar to those reported for other XFs.[3b] Contrary to some of the other XFs, **5** is fully planarized in the solid state and forms tilted stacks, typical for aromatic hydrocarbons, where direct $\pi-\pi$ stacking between the aromatic systems is avoided.[12] In this packing motif, the butyl groups act as molecular insulation.

Spectroscopic Properties and Quantum Chemical Calculations. All of the isolated phenothiazine XFs form brightly yellow-orange fluorescent solutions in dichloromethane. Figure 3 shows the absorption and emission spectra of XFs **5**−**9**. The absorption spectra of XF **6**−**9** are similar and show a significant charge-transfer band at around 430−450 nm and a second more intense absorption at around 325 nm. This charge-transfer band is absent in the all-donor-substituted XF **5**; it displays a single broad band with a maximum absorption at 392 nm.[13]

(11) Horner, L.; Hoffmann, H.; Wippel, H. G.; Klahre, G. *Chem. Ber.* **1959**, *92*, 2499−2505.

(12) Hunter, C. A.; Sanders, J. K. M. *J. Am. Chem. Soc.* **1990**, *112*, 5525−5534.

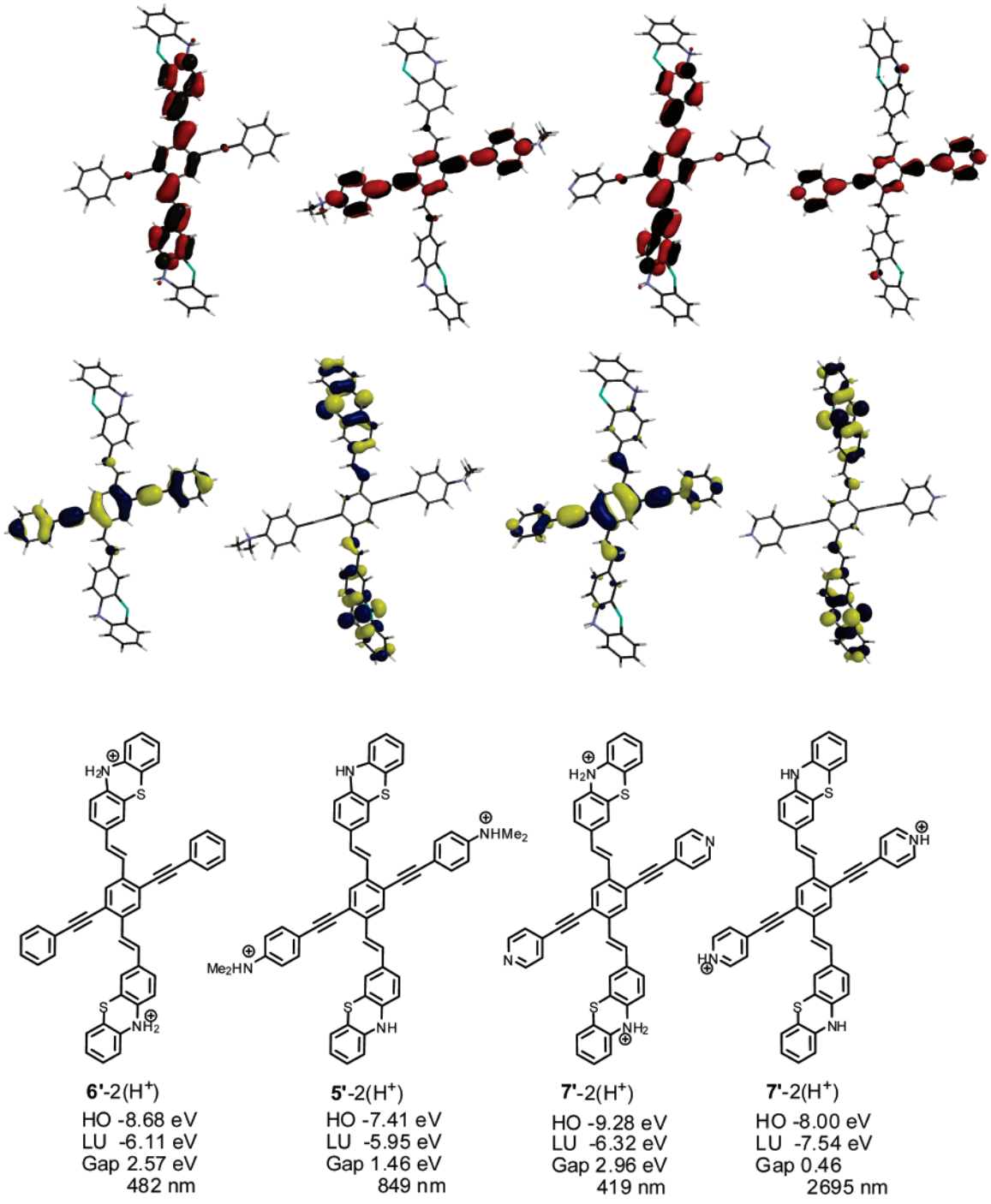

FIGURE 5. Molecular orbital plots (LUMOs, top; HOMOs, bottom) of the bisprotonated species **5′**-$(2H)^+$, **6′**-$(2H)^+$, and **7′**-$(2H)^+$. The calculations were performed using B3LYP/6-31G*//6-31G* as implemented on SPARTAN.

The emission spectra of the XFs are broad and featureless and range from 552 to 590 nm. The donor-substituted XF **5** possesses the highest energy emission. Increasing donor−acceptor strength substitution leads to increasing red shift of the fluorescence of the XFs. Table 1 shows spectroscopic data for **6**−**9** including the quantum yield. Increasing donor−acceptor substitution also decreases the quantum yields of the XFs, in good qualitative agreement with the energy gap law.[14] In order to rationalize the charge-transfer band present in **6**−**9**, we performed quantum chemical calculations (B3LYP/6-31G*//6-31G*) on smaller model systems **5′**−**7′** that omitted the *N*-hexyl groups on the phenothiazine unit. Figures 4 and 5 show repre-

(13) The .cif file containing the crystallographic data for **5** is available as part of the electronic Supporting Information. This data may be viewed using the Mercury software available free of charge from the Cambridge Crystallographic Data Centre (http://www.ccdc.cam.ac.uk/).

(14) (a) Tolbert, L. M.; Nesselroth, S. M.; Netzel, T. L.; Raya, N.; Stapleton, M. *J. Phys. Chem.* **1992**, *96*, 4492−4496. (b) Englman, R.; Jortner, J. *Mol. Phys.* **1970**, *18*, 145−154. (c) Caspar, J. V.; Meyer, T. J. *J. Phys. Chem.* **1983**, *87*, 952−957.

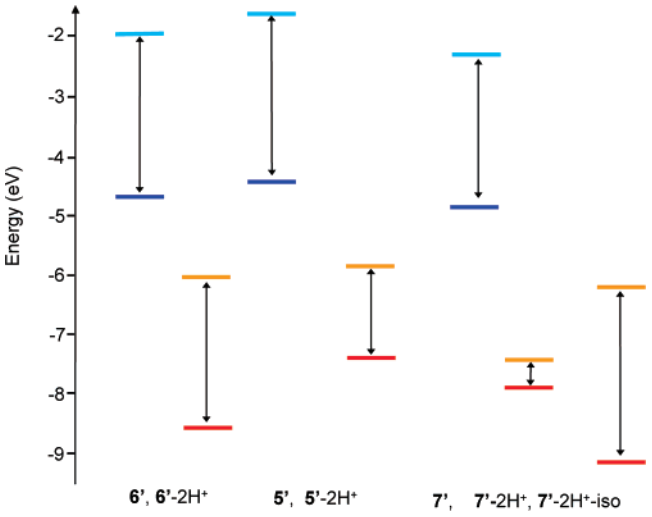

FIGURE 6. Absolute HOMO−LUMO positions from B3LYP/6-31G*//6-31G* calculations.

sentations of the HOMO and the LUMO of simplified versions of **5**−**7**, viz. **5′**−**7′** in their neutral and doubly protonated forms. Figure 6 shows the calculated orbital positions.

We have recently shown that in XFs, HOMO and LUMO can localize on the distyrylbenzene and the arylethynyl axis, respectively, if the transverses are donor- and acceptor-substituted (Figure 1).[3,15] It was of interest to see if the same type of "disjoint" orbital arrangement could also be observed in **5**−**7**. Inspection of the FMOs of **5′**−**7′** shows that there is some spatial separation between the FMOs but not as significant as in the case of simpler XFs such as **10** and **11**. In the donor-substituted **5′**, we do not observe spatial separation of the FMOs. Only in **7′** is clear FMO separation enforced by the substituents; the bis(vinylphenothiazine)benzene axis in **7′** is electron-rich, whereas the bis(pyridylethynyl)benzene axis has an electron-accepting character. While **5′** and **6′** have a more congruent orbital structure,[3,15] it might be possible to induce the "diagonalization" of the FMOs of the C-class XFs **5** and **6** upon protonation and/or addition of metal salts. We therefore computationally investigated the protonation of **5′**−**7′**. Figures 5 and 6 show the details. In the case of **6′**, protonation of the phenothiazines leads to a species with a disjoint FMO structure. The HOMO of **6′**-2H$^+$ is located on the bis(arylethynyl) axis, while the LUMO is located on the axis containing the protonated phenothiazines. While these calculations forecast a dramatically different FMO structure, they do not predict an increase in the band gap upon protonation. However, this level of theory may not be sufficient to project spectroscopic changes. In **5**, we expect that the alkylanilines would be protonated preferentially. As a consequence, we computed **5′**-2H$^+$, in which the aniline nitrogens in **5′** are protonated. In the case of **7′**, we investigated the protonation of the pyridine units and also protonation of the phenothiazines.

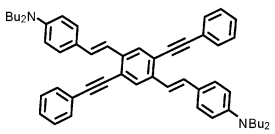

10

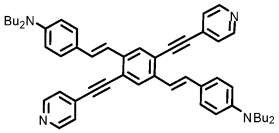

11

In the case of **5′**, which is all-donor-substituted, protonation of the aniline nitrogens leads to a decrease in the HOMO−LUMO gap and the development of a disjoint orbital structure, in which the anilinium ions are the acceptors and the phenothiazine-containing axis localizes the HOMO. When the phenothiazine units of **7** are protonated, the HOMO is localized on the bis(pyridinylethynyl)benzene axis, while the LUMO is localized on the axis that contains the protonated phenothiazines. A blue shift of the emission is expected (and found experimentally, vide infra), due to the increase in the HOMO−LUMO gap by removing the donor character from the phenothiazine transverse. Upon protonation of the pyridine, the already pronounced spatial HOMO−LUMO separation in **7′** is further amplified and becomes extreme to such a point that there is no Franck−Condon overlap between the FMOs anymore. At the same time, the HOMO−LUMO gap shrinks to 0.46 eV. Similar, but lesser, red and blue shifts are observed in elongated oligo(phenylene-ethynylene)s, also due to a lessening of FMO overlap.[8d]

Titration Studies of 5−7 Using Trifluoroacetic Acid in Dichloromethane. To see if the qualitative predictions of the quantum chemical calculations were correct, we performed titration studies on **5**−**7**. Generally, the protonation of phenothiazine forms oxidized radical cations.[9,16] In our hands (vide infra), protonation with a strong acid leads to a spectroscopic behavior that is best interpreted by partial oxidation but mostly simple multiple protonation of the phenothiazine nuclei. We investigated the absorption and the emission of **5**−**7** in the presence of increasing amounts of trifluoroacetic acid in

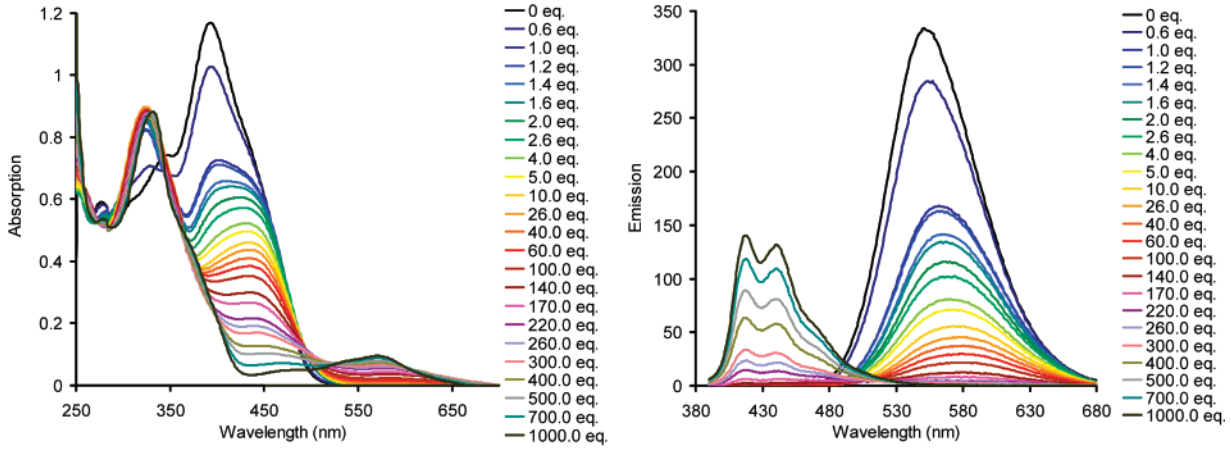

FIGURE 7. Absorption and emission spectra of XF **5** in the presence of increasing amounts of TFA.

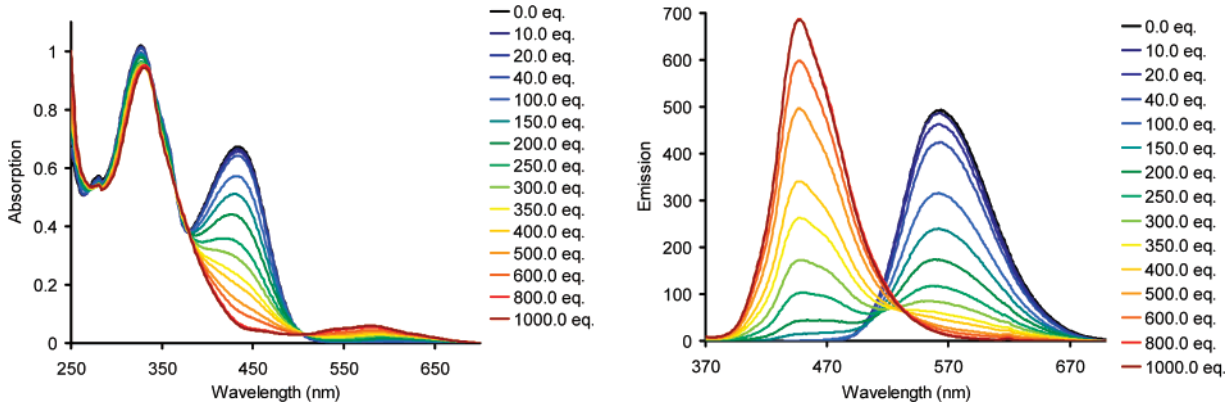

FIGURE 8. Absorption and emission spectra of XF **6** in the presence of increasing amounts of TFA.

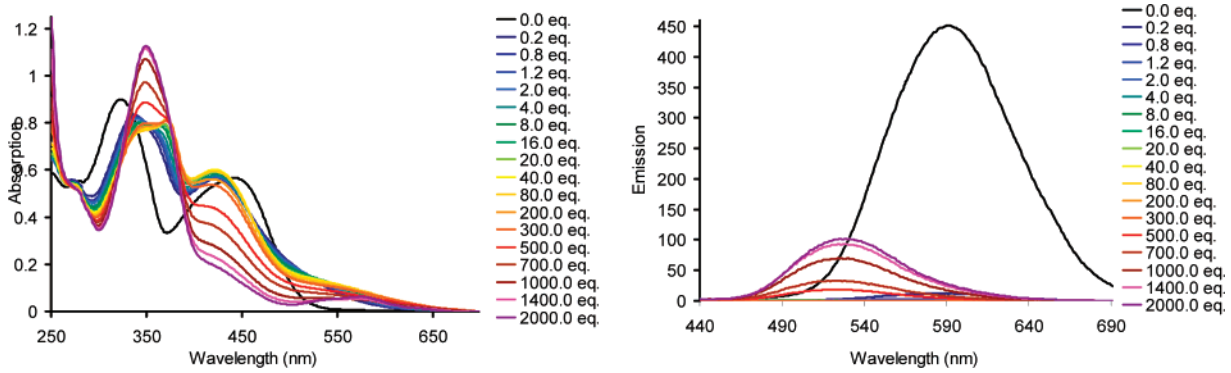

FIGURE 9. Absorption and emission spectra of XF **7** in the presence of increasing amounts of TFA.

dichloromethane. The spectra of the titration experiments are shown in Figures 7−9. The simplest case is that of **6** (Figure 8), where only the phenothiazine groups are present as basic sites. Upon addition of up to 40 equiv of TFA, there is no change in the absorption spectrum and only a small decrease in fluorescence intensity. After addition of 250 equiv of TFA, there are two bands of approximately equal height visible in the emission spectrum. One is the original band recorded at 563 nm, while the second band is a blue-shifted feature at 447 nm. Upon increasing the amount of TFA, the absorption feature located at 433 nm decreases and a somewhat blue-shifted maximum develops at 331 nm. After the addition of 1000 equiv of TFA, the protonation is complete and only the blue emitting feature at 447 nm remains. In the absorption spectra, a band grows in at around 590 nm upon exposure of **6** to large amounts of TFA under air. We see this secondary peak developing at 550−600 nm in all of the phenothiazine XFs when they are exposed to a large excess of TFA in air. This absorption band is most probably a consequence from some oxidation of the XFs to the respective radical cations on each of the phenothiazine sites. The oxidation of phenothiazines in acidic solution is not uncommon and has been discussed.[16] However, complete oxidation of the XF is unlikely, as we have a strong blue fluorescence that is located at higher energy than the absorption maximum for the secondary band in absorption. In addition, a phenothiazine radical cation would in all probability be nonfluorescent. The presence of some percentage of radical cations is supported by the massive broadening and downfield shift of the proton NMR signals upon the addition of a large excess of TFA.

Overall, this spectroscopic behavior can be interpreted by considering the FMO arrangement of **6**. Upon protonation of the phenothiazine rings, the HOMO of **6** is substantially stabilized while the LUMO is less affected. As a consequence, the observed blue shift in emission and the disappearance of the absorption feature at 433 nm are not unexpected. These spectroscopic properties are similar to those reported for the dibutylamino XF **10**, only that the corresponding transitions in **10** are red shifted and that the protonation of the phenothiazine units is considerably more difficult than that of the dibutylanilines in **10**. Our inability to forecast the increase in the HOMO−LUMO gap of **6** upon protonation using the model compound **6′** using a B3LYP/631G*//6-31G* calculation is probably due to the relatively low level of theory we have to employ in these relatively large molecules.

After addition of 10 equiv of TFA to a solution of **5**, the feature recorded at 392 nm diminishes in intensity and centers at 432 nm. At the same time, we observe a shift in the emission from 552 to 577 nm. We attribute these changes to the protonation of the dibutylaniline moieties in **5**. Under these conditions, we transform **5** into **5**-2H$^+$, a donor−acceptor species with a disjoint FMO structure and a decreased band gap. Upon addition of considerably more TFA (1000 equiv), the phenothiazine units are also protonated. Both the absorption and the emission are blue shifted as the HOMO is now stabilized by the protonation of the phenothiazine nuclei, yet the LUMO does not seem to be affected. Again, the broad feature that

(15) Fahrni, C. J.; Yang, L. C.; VanDerveer, D. G. *J. Am. Chem. Soc.* **2003**, *125*, 3799−3812.

(16) (a) Pankratov, A. N.; Uchaeva, I. M.; Stepanov, A. N. *Can. J. Chem.* **1993**, *71*, 674−677. (b) Kamenov, L. L.; Simov, D.; Golubev V. B. *Theor. Exp. Chem.* **1971**, 115−118.

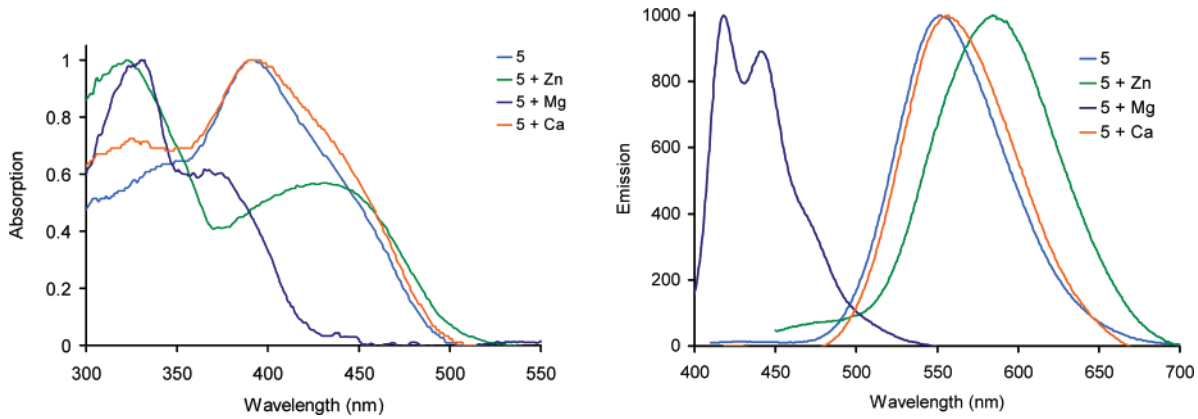

FIGURE 10. Absorption and emission spectra of XF **5** in the presence of different metal cations. Spectra in Figures 10−14 are normalized for absorption to 1.00 and for emission to 1000.

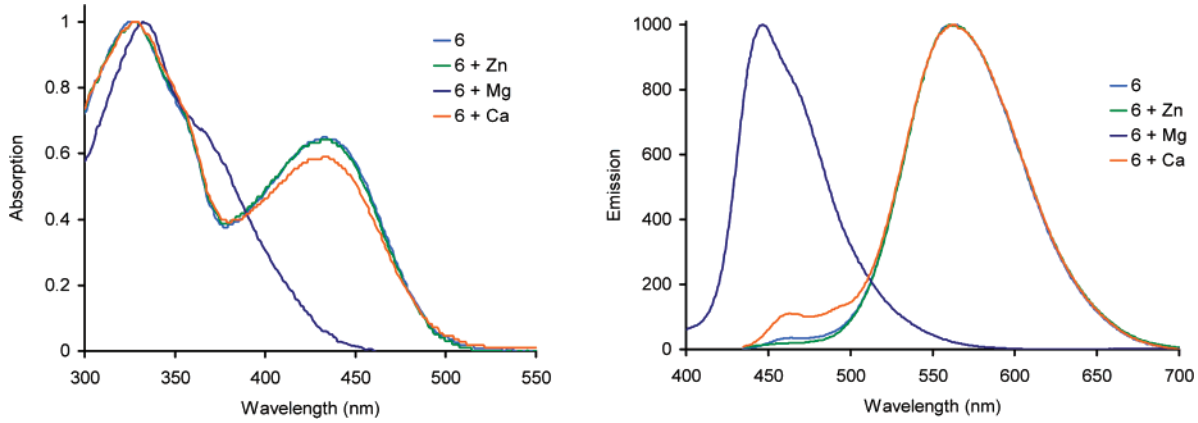

FIGURE 11. Absorption and emission spectra of XF **6** in the presence of different metal cations.

emerges at around 600 nm in the absorption spectrum is attributed to the partial oxidation of the phenothiazine units under these conditions.

In the case of **7**, the neutral compound displays an absorption at 442 nm (Figure 9). Addition of up to 40 equiv of TFA leads to a red shift in absorption that is characterized by a shoulder/tail at 550 nm and a sharp peak at 422 nm. We assign this signature to the doubly pyridine-protonated XF **7**. Upon further addition of TFA, the shoulder disappears and the feature at 350 nm dominates the absorption spectrum. A second red-shifted, weak but distinct band appears at >550 nm, suggesting partial oxidation of the phenothiazine nucleus. The main emission of **7** at 589 nm is quenched after the addition up to 100 equiv of TFA. Upon addition of more TFA, a new blue-shifted emission is observed at 528 nm. We assume that first the pyridine units are protonated, leading to a species with a very low band gap, as the LUMO is stabilized by protonation. This species is nonfluorescent as there apparently are effective paths available for nonradiative excited-state deactivation, in line with the energy gap law.[15] Upon further addition of TFA, the phenothiazine units are likewise protonated, stabilizing the HOMO. An all-acceptor-substituted species with congruent FMOs displaying an increased HOMO−LUMO gap results. The **7**-4H$^+$ tetracation is fluorescent and would be best described as a class C cruciform.

Interaction of the XFs with Metal Salts. The study of the interaction of **5**−**7** with TFA was illuminating: Absorption and emission of the XFs are manipulated by protonation. It was of interest if similar effects could be elicited by the addition of metal cations to the XFs. We investigated both the absorption and the emission of **5**−**9** (Figures 10−14) in the presence of Mg^{2+}, Zn^{2+}, and Ca^{2+} in form of their triflates in dichloromethane solution. From prior experience, we are expecting that the binding affinity for the anilines, pyridines, and phenothiazines would be $Mg^{2+} > Zn^{2+} \gg Ca^{2+}$.[3] Zinc complexes with promazine hydrochlorides had been proposed by Gowda et al. The coordination of zinc chloride with the phenothiazinyl sulfur was inferred from shifts of C−S valence bands in the IR spectra.[17] However, prominent effects in the electronic spectra of the complexes were not observed.

TABLE 2. Absorption and Emission Spectra of 5−9 in the Presence of Divalent Metal Ions

solvent: dichloromethane	**5**	**6**	**7**	**8**	**9**
λ_{max} abs (nm)	392	433	442	437	433
λ_{max} abs (nm) + Zn^{2+}	431	433	412	440	444
λ_{max} abs (nm) + Mg^{2+}	369 sh	371 sh	431 sh	362	371
	330	332	348	328	329
λ_{max} abs (nm) + Ca^{2+}	392	433	437	440	439
λ_{max} emission (nm)	552	563	589	579	590
λ_{max} emission (nm) + Zn^{2+}	586	561	quenched	579	594
λ_{max} emission (nm) + Mg^{2+}	418	447	513	420	415
	441			443	437
λ_{max} emission (nm) + Ca^{2+}	557	564	592	579	590

The exposure of **5** to $Ca(OTf)_2$ in dichloromethane (Figure 10, Table 2) elicits a vanishingly small bathochromic shift in

(17) Gowda, N. M. M.; Pacquette, H. L.; Kim, D.-H.; Jayaram, B. *J. Mol. Struct.* **1996**, *382*, 129−135.

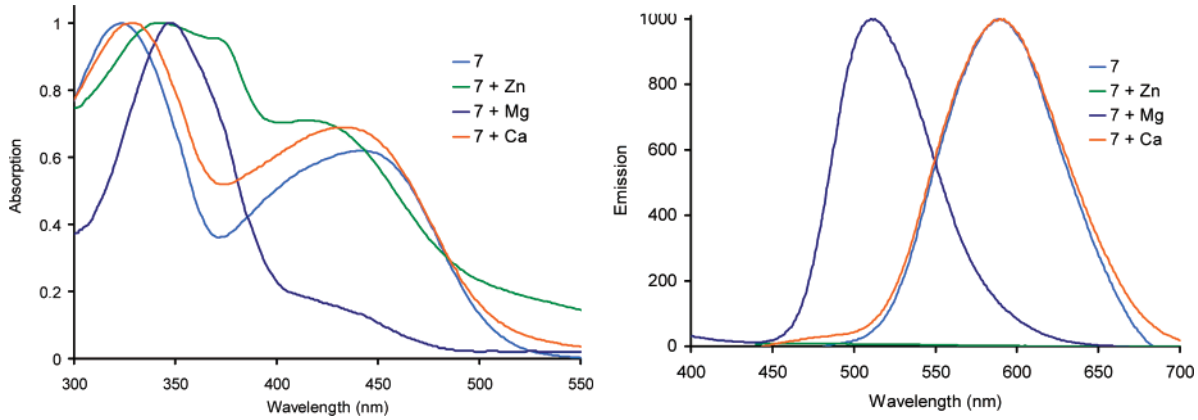

FIGURE 12. Absorption and emission spectra of XF **7** in the presence of different metal cations.

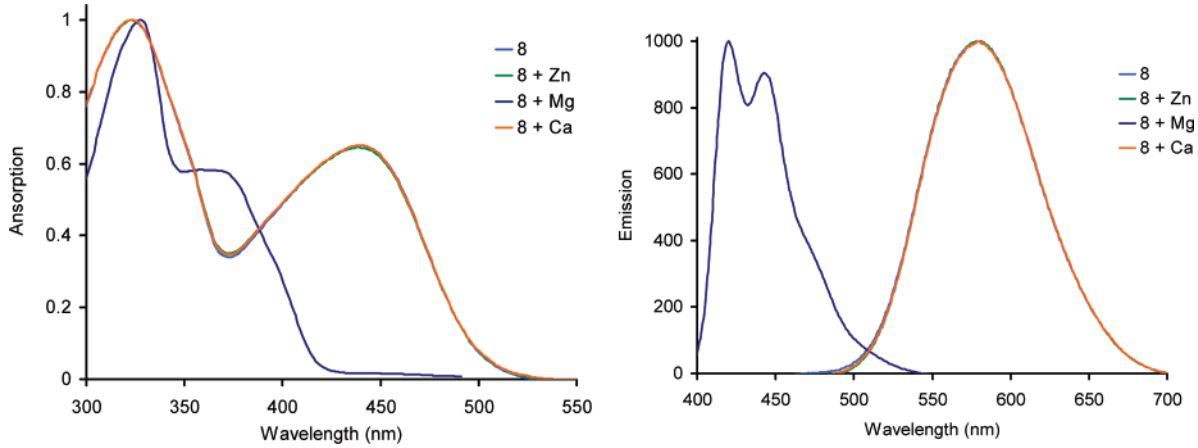

FIGURE 13. Absorption and emission spectra of XF **8** in the presence of different metal cations.

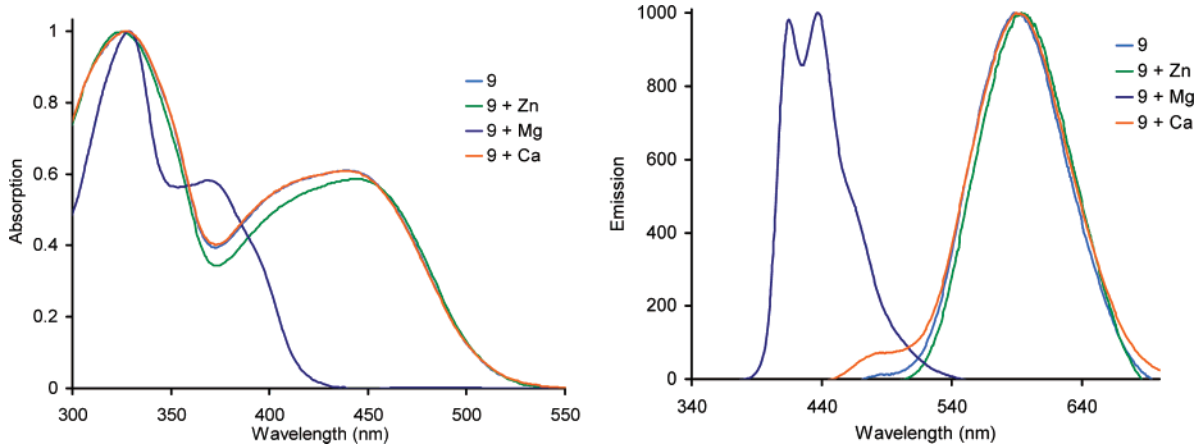

FIGURE 14. UV−vis and emission spectra of XF **9** in the presence of different metal cations.

absorption and emission, probably due to weak binding. In the case of $Zn(OTf)_2$, a striking red shift in both absorption and emission is observed, while $Mg(OTf)_2$ causes a blue shift in both emission and absorption. The differences in the spectroscopic behavior can be easily explained if one assumes that $Zn(OTf)_2$ binds to the dibutylanilines but does *not* bind to the phenothiazine nuclei, transforming the donor XF **5** into a donor−acceptor XF with a decreased band gap. The arylethynyl transverse localizes the LUMO after zinc coordination, while the HOMO is still localized on the phenothiazine-bearing axis. The binding affinity of $Mg(OTf)_2$ is sufficiently high to coordinate not only to the dibutylanilines but also to the phenothiazine nuclei, transforming the donor-substituted XF **5** into an all-acceptor-substituted XF with an increased band gap. In this case, the HOMO is more stabilized than the LUMO to give the blue emitting species.

In the case of **6** (Figure 11), $Ca(OTf)_2$ and $Zn(OTf)_2$ give insignificant responses, while coordination of $Mg(OTf)_2$ induces blue shift in both absorption and emission. XF **6** is a model compound for both **5** and **7** in the sense that it only contains the phenothiazine moieties and therefore displays an easier to interpret change in photophysics upon metal salt coordination.

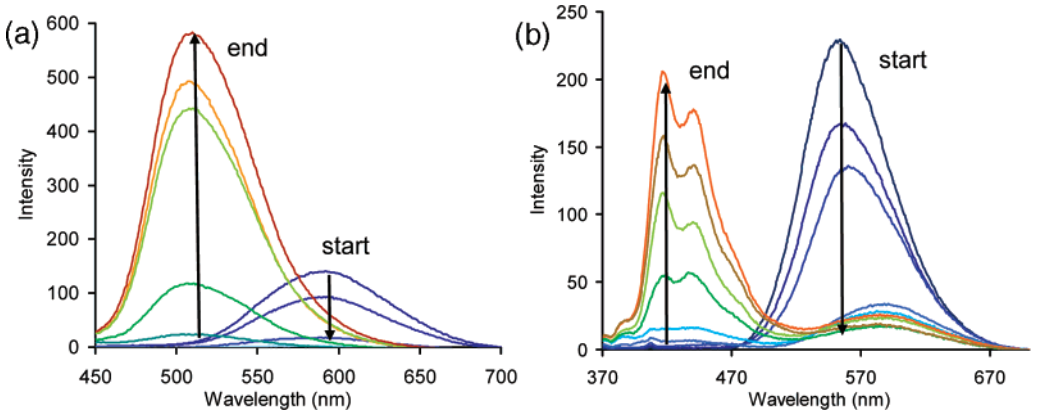

FIGURE 15. (a) Interaction of **7** with increasing amount of $Mg(OTf)_2$, and (b) interaction of XF **5** with increasing amounts of $Mg(OTf)_2$. Arrows show increasing concentration of $Mg(OTf)_2$.

In the cases of **8** and **9**, which are in effect only acceptor-substituted variants of **7**, the same coordination pattern as in **6** is observed with all three metal triflates.

The XF **7** is structurally reminiscent of the donor−acceptor XF **11**. Are the same spectroscopic effects observed in **7**? In **11**, we find a blue shift in both emission and absorption when treating with either $Zn(OTf)_2$ or $Mg(OTf)_2$.[3] Upon addition of an excess of these salts, we see a second, bathochromic shift that leads to a green emissive species as the end point. We contend that the dibutylanilines are coordinated first, leading to a stabilization of the HOMO. The subsequent coordination of the metal salt to the pyridines stabilizes the LUMO. Figure 12 shows the exposure of **7** to metal triflates: $Ca(OTf)_2$ unsurprisingly does not coordinate. Upon addition of $Zn(OTf)_2$, we see a red shifted but very broad absorption that is tailing beyond 600 nm, *while the emission of this species is quenched*. Upon addition of $Mg(OTf)_2$ to the solution of **7**, a significant blue shift is observed both in absorption and emission. The spectral changes induced by $Mg(OTf)_2$ are very similar to those observed upon addition of an excess of TFA to **5**−**7**, while the spectral changes observed upon addition of $Zn(OTf)_2$ to the cruciforms resemble those observed upon protonation of the non-phenothiazine nitrogens.

The behavior of **7** when compared to **11** is inverted with respect to the coordination ability of the ligands on the XF transverses. In **7**, the pyridines coordinate stronger than the phenothiazines, and the addition of $Zn(OTf)_2$ leads to a highly disjoint XF with a very small HOMO−LUMO gap. The decrease of the Franck−Condon overlap in combination with the energy gap law[14] leads to a disallowed HOMO−LUMO transition; radiationless deactivation of the excited state occurs and quenching is observed. In the case of the stronger coordinating $Mg(OTf)_2$, all four binding sites are occupied by metal ions and an all-acceptor-substituted class C XF with a strong emission in the green results. To exclude the possibility that $Mg(OTf)_2$ does only coordinate with two of the four sites, we performed a titration of **7**, which is shown in Figure 15a. Upon addition of a small amount of a saturated solution of $Mg(OTf)_2$ to the XF, the fluorescence is quenched. Upon addition of more $Mg(OTf)_2$, a strong emission centered at 512 nm develops. The same type of titration can also be performed with **5**, as shown in Figure 15b. Here also the fluorescence red shifts and weakens considerably when a small amount of a $Mg(OTf)_2$ is added, suggesting that only the dialkylaniline units are coordinated. Upon further addition of $Mg(OTf)_2$, the expected

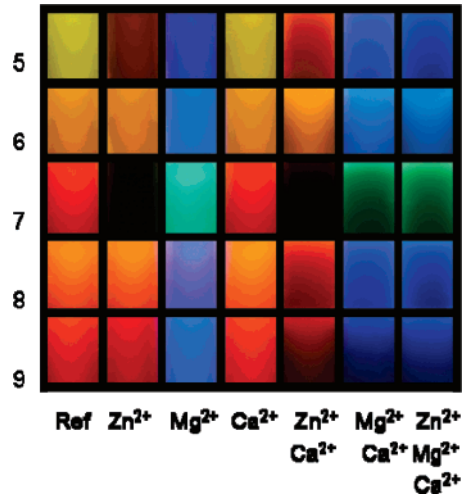

FIGURE 16. Exposure of the XFs **5**−**9** to different metal ions. The picture is taken on a black background using a hand-held UV lamp with a λ_{max} of emission at 365 nm and represents the metallochromic properties of the XFs in emission quite well.

blue emission appears as all four sites are coordinated. Our results suggest contrary to literature claims that Zn^{2+} does not strongly coordinate to phenothiazine, even if zinc triflate is used in a weakly coordinating solvent such as dichloromethane.[17]

Conclusions

In conclusion, we have prepared five XFs **5**−**9** containing phenothiazine moieties on the arylenevinylene transverse. Depending upon their substitution pattern, these XFs show either class C (congruent) or class D (disjoint) FMOs.[3] Exposure of these XFs to either trifluoroacetic acid or to metal salts leads to strong chromic effects in absorption and in emission.[18] A small panel of these XFs allows us to visualize the observed metallochromic effects and demonstrates that such simple responsive fluorophores can discern zinc from magnesium ions without the interference of calcium ions, as shown in Figure 16. The coordinative ability of $Ca^{2+} < Zn^{2+} < Mg^{2+}$ explains the observed changes in emission and absorption. Quantum

(18) (a) Henary, M. M.; Wu, Y. G.; Fahrni, C. J. *Chem.—Eur. J.* **2004**, *10*, 3015−3025. (b) Pond, S. J. K.; Tsutsumi, O.; Rumi, M.; Kwon, O.; Zojer, E.; Bredas, J. L.; Marder, S. R.; Perry, J. W. *J. Am. Chem. Soc.* **2004**, *126*, 9291−9306.

chemical model calculations support the observed trends. When compared to the "classic" XFs such as **10** or **11**, the incorporation of the aniline nitrogens into the phenothiazine framework decreases their basicity and metal coordinating ability as would be expected from simple hybridization and resonance arguments. The herein presented XFs display a significantly different pattern of metallochromicity as compared to those observed in **10** and **11**.

In the future, we will prepare water-soluble and ligand-appended derivatives of **5**−**9** and investigate their metallochromic behavior upon addition of transition metal salts to explore if the two-stage emission modulation is broadly applicable and useful.

Experimental Section

3,3′-(1*E*,1′*E*)-2,2′-(2,5-Diiodo-1,4-phenylene)bis(ethene-2,1-diyl)bis(10-hexyl-10*H*-phenothiazine) 4. An oven-dried Schlenk flask cooled under nitrogen atmosphere was charged with dry THF (50 mL), diphosphonate **3** (788 mg, 1.25 mmol), and NaH (33.0 mg, 1.38 mmol) until the solution turned a purple-red color. Aldehyde **2** (973 mg, 3.13 mmol) was added to the stirred mixture. The color changed to orange, and a solid precipitated. The reaction mixture was stirred overnight at room temperature. The reaction was quenched with water. Dichloromethane (200 mL) was added and extracted five times with brine and dried over magnesium sulfate. The solvent was evaporated under reduced pressure. The resulting solid was crystallized from dichloromethane/hexanes yielding 1.06 g (1.12 mmol, 90%) of bright orange crystals of **4**: mp 178−180 °C; ^{1}H NMR (300 MHz, CD_2Cl_2) δ 0.85−0.91 (m, 6H), 1.28−1.34 (m, 8H), 1.39−1.48 (m, 4H), 3.85 (t, 4H, J = 7.2 Hz), 6.83−6.95 (m, 8H), 7.04 (d, 2H, J = 16.0 Hz), 7.12 (dd, 2H, J = 1.5, 7.6 Hz), 7.14−7.19 (m, 2H), 7.29−7.34 (m, 4H), 8.06 (s, 2 H); ^{13}C NMR (75.5 MHz, CD_2Cl_2) δ 14.2, 23.0, 26.9, 27.1, 31.8, 47.9, 100.6, 115.7, 115.8, 122.8, 124.2, 125.16, 125.17, 125.4, 126.8, 127.6, 127.7, 128.8, 131.3, 136.3, 140.8, 145.0, 145.6; IR (KBr) $\tilde{\nu}$ [cm^{-1}] 2953 (m), 2927 (m), 2854 (w), 1625 (m), 1599 (m), 1575 (m), 1495 (m), 1467 (s), 1443 (s), 1404 (w), 1364 (w), 1335 (w), 1290 (w), 1247 (m), 1208 (w), 1041 (m), 955 (m), 746 (m); UV/vis (CH_2Cl_2) λ_{max} (ϵ) 250 nm (60000), 276 nm (39000), 328 nm (36000), 424 nm (50000); emission (CH_2Cl_2) λ_{max} 578 nm; MS (FAB$^+$) (*m*/*z* (%)) 945 (M − H$^+$, 66), 944 (M$^+$, 100), 899 (10), 898 (13), 896 (13), 873 (10), 860 (14), 859 (17); HRMS calcd for $C_{46}H_{46}I_2N_2S_2$ 944.1192, found 944.1168.

4,4′-(2,5-Bis((*E*)-2-(10-hexyl-10*H*-phenothiazin-3-yl)vinyl)-1,4-phenylene)bis(ethyne-2,1-diyl)bis(*N*,*N*-dibutylbenzenamine) 5. In an oven-dried Schlenk tube cooled under nitrogen atmosphere, **4** (300 mg, 0.317 mmol) was dissolved in dry THF (8 mL), piperidine (1 mL), and ethanol (2 mL) and combined with $PdCl_2(PPh_3)_2$ (4.5 mg, 6.4 μmol, 2 mol %) and CuI (2.4 mg, 13 μmol, 4 mol %). *N*,*N*-Dibutyl-4-((trimethylsilyl)ethynyl)aniline (241 mg 0.799 mmol) and potassium hydroxide (157 mg 2.80 mmol) were added, and the reaction was started with a heat gun. Salts started to precipitate immediately. The reaction mixture was stirred overnight at room temperature. The crude mixture was diluted with dichloromethane and washed three times with water, three times with brine, and once with aqueous ammonia hydroxide solution. The organic phase was dried with magnesium sulfate and evaporated under reduced pressure. The product was purified by column chromatography using hexanes/ethyl acetate (9:1) and crystallization from dichloromethane/hexanes to give **5** (223 mg, 0.19 mmol, 61%) as orange crystals suitable for crystallographic analysis: mp 162−166 °C; ^{1}H NMR (300 MHz, CD_2Cl_2) δ 0.86−0.92 (m, 6H), 1.00 (t, 12H, J = 7.3 Hz), 1.26−1.49 (m, 20H), 1.55−1.69 (m, 8H), 1.74−1.88 (m, 4H), 3.29−3.38 (m, 8H), 3.86 (t, 4H, J = 7.1 Hz), 6.68 (d, 4H, J = 8.7 Hz), 6.88−6.93 (m, 6H), 7.10−7.20 (m, 6H), 7.32−7.41 (m, 4H), 7.50 (d, 4H, J = 8.5 Hz), 7.57 (d, 2H, J = 16.3 Hz), 7.82 (s, 2H); ^{13}C NMR (75.5 MHz, CD_2Cl_2) δ 14.1, 20.2, 23.0, 26.9, 27.1, 29.7, 31.8, 47.9, 51.0, 86.2, 97.5, 108.6, 111.6, 115.75, 115.77, 122.6, 122.7, 124.4, 125.1, 125.5, 126.3, 127.57, 127.60, 128.3, 129.0, 132.3, 133.1, 133.2, 136.9, 145.18, 145.19, 148.6; IR (KBr): $\tilde{\nu}$ [cm^{-1}] 2955 (s), 2929 (s), 2869 (m), 2858 (m), 2192 (m), 1604 (s), 1521 (s), 1496 (m), 1465 (m), 1445 (s), 1402 (m), 1367 (m), 1336 (m), 1289 (m), 1247 (m), 1223 (m), 1193 (m), 812 (m), 746 (m); UV/vis (CH_2Cl_2) λ_{max} (ϵ) 252 nm (40000), 278 nm (36000), 312 nm (45000), 348 nm (56000), 391 nm (90000), 450 nm (47000); emission (CH_2Cl_2) λ_{max} (ϵ) 552 nm; MS (FAB$^+$) (*m*/*z* (%)) 1149 (24), 1148 (56), 1147 (M − H$^+$, 95), 1146 (M$^+$, 100), 1145 (34); HRMS calcd for $C_{78}H_{90}N_4S_2$ 1146.6607, found 1146.6631.

3,3′-(1*E*,1′*E*)-2,2′-(2,5-Bis((4-*tert*-butylphenyl)ethynyl)-1,4-phenylene)bis(ethene-2,1-diyl)bis(10-hexyl-10*H*-phenothiazine) 6. An oven-dried Schlenk flask cooled under nitrogen atmosphere was charged with dry THF (5 mL) and piperidine (3 mL); diiodide **4** (200 mg, 0.211 mmol) was dissolved and combined with $PdCl_2(PPh_3)_2$ (3.0 mg, 4.2 μmol, 2 mol %) and CuI (1.6 mg 8.4 μmol, 4 mol %). The reaction mixture was stirred for 15 min before 1-*tert*-butyl-4-ethynylbenzene (83.1 mg 0.53 mmol) was added. After a few minutes, salts started to precipitate. The reaction was stirred at room temperature overnight. The crude reaction mixture was diluted with dichloromethane, and the organic phase was washed three times with water, two times with brine, and two times with 5% aqueous ammonia hydroxide solution, dried with magnesium sulfate, and concentrated under vacuum. The product was first purified via column chromatography and then via recrystallization from dichloromethane/hexanes yielding **6** (63.0 mg, 0.06 mmol, 30%) as a yellow powder: mp 216−218 °C; ^{1}H NMR (300 MHz, CD_2Cl_2) δ 0.85−0.92 (m, 6H), 1.28−1.40 (m, 24H), 1.40−1.49 (m, 4H),1.81 (td, 4H, J = 7.6, 14.8 Hz), 3.86 (t, 4H, J = 7.2 Hz), 6.84−6.96 (m, 6H), 7.10−7.23 (m, 6H), 7.32−7.40 (m, 4H), 7.50−7.62 (m, 6H), 7.87 (s, 2H); ^{13}C NMR (75.5 MHz, CD_2Cl_2) δ 14.1, 23.0, 26.9, 27.1, 31.3, 31.8, 35.2, 47.9, 87.5, 96.0, 115.8, 120.3, 122.4, 122.8, 124.0, 124.4, 125.2, 125.6, 125.9, 126.0, 126.4, 127.59, 127.64, 128.8, 129.6, 131.6, 132.0, 137.5, 145.1, 145.4, 152.5; IR (KBr) $\tilde{\nu}$ [cm^{-1}] 2985 (m), 2929 (m), 2867 (w), 2858 (w), 1629 (m), 1603 (w), 1575 (w), 1515 (w), 1497 (w), 1466 (s), 1444 (s), 1364 (w), 1335 (w), 1269 (m), 1248 (w), 959 (w), 746 (w), 562 (w); UV/vis (CH_2Cl_2) λ_{max} (ϵ) 242 nm (48000), 280 nm (37000), 328 nm (89000), 358 (60000), 433 nm (60000); emission (CH_2Cl_2) λ_{max} 563 nm; MS (FAB$^+$) (*m*/*z* (%)) 1008 (22), 1007 (48), 1006 (M − H$^+$, 81), 1005 (M$^+$, 100), 1004 (22), 921 (10), 919 (13); HRMS calcd for $C_{70}H_{72}N_2S_2$ 1004.5137, found 1004.5092.

3,3′-(1*E*,1′*E*)-2,2′-(2,5-Bis(pyridin-4-ylethynyl)-1,4-phenylene)-bis(ethene-2,1-diyl)bis(10-hexyl-10*H*-phenothiazine) 7. In an oven-dried Schlenk tube cooled under nitrogen atmosphere, **4** (300 mg, 0.317 mmol) was dissolved in dry THF (6 mL) and piperidine (1 mL) and combined with $PdCl_2(PPh_3)_2$ (4.5 mg, 6.4 μmol, 2 mol %) and CuI (2.4 mg, 13 μmol, 4 mol %). 4-((Triisopropylsilyl)-ethynyl)pyridine (208 mg, 0.80 mmol) was added via syringe, and the reaction was started by the addition of tetrabutylammonium fluoride solution (230 mg, 0.88 mmol, 1 M in THF). Salts started to precipitate immediately, and the color changed from bright orange to red/brown. The reaction mixture was stirred overnight at room temperature. The crude mixture was diluted with dichloromethane and washed three times with water, three times with brine, and once with aqueous ammonia hydroxide solution. The organic phase was dried with magnesium sulfate and evaporated under reduced pressure. The product was purified by recrystallization from dichloromethane/hexanes yielding **7** (176 mg, 0.20 mmol, 61%) as an orange-red solid: mp 186−190 °C; ^{1}H NMR (300 MHz, CD_2Cl_2) δ 0.84−0.93 (m, 6H), 1.25−1.36 (m, 8H), 1.38−1.50 (m, 4H), 1.74−1.86 (m, 4H), 3.85 (t, 4H, J = 7.1 Hz), 6.84−6.97 (m, 6H), 7.09−7.21 (m, 6H), 7.29−7.37 (m, 4H), 7.40−7.51 (m, 6H), 7.88 (s, 2H), 8.64 (s, 4H); ^{13}C NMR (75.5 MHz, CD_2Cl_2) δ 14.1, 23.0, 26.9, 27.1, 31.8, 47.9, 92.1, 93.2, 115.8, 115.9, 122.0, 122.9, 123.2, 124.3, 125.3, 125.6, 125.7, 126.5, 127.6, 127.7, 129.3, 130.4, 131.2, 131.6, 137.9, 145.0, 145.7, 150.3; IR (KBr) $\tilde{\nu}$ [cm^{-1}] 3553 (s), 3548

(s), 3511 (s), 3495 (s), 3456 (s), 3447 (s), 3442 (s), 3436 (s), 3431 (s), 3426 (s), 3420 (s), 3267 (m), 2967 (m), 2957 (w), 2928 (m), 2857 (w), 2207 (w), 1628 (m), 1591 (s), 1575 (w), 1497 (m), 1467 (s), 1443 (w), 1249 (m); UV/vis (CH_2Cl_2) λ_{max} (ϵ) 250 nm (43000), 300 nm (58000), 326 nm (78000), 442 nm (51000); emission (CH_2Cl_2) λ_{max} 589 nm; MS (FAB$^+$) (*m*/*z* (%)) 897 (28), 896 (54), 895 (M − H$^+$, 100), 894 (M$^+$, 90), 893 (17), 810 (15); HRMS calcd for $C_{60}H_{54}N_4S_2$ 894.3790, found 894.3802.

3,3′-(1*E*,1′*E*)-2,2′-(2,5-Bis((3-(trifluoromethyl)phenyl)ethynyl)-1,4-phenylene)bis(ethene-2,1-diyl)bis(10-hexyl-10*H*-phenothiazine) 8. In an oven-dried Schlenk tube cooled under nitrogen atmosphere, **4** (300 mg, 0.317 mmol) was dissolved in dry THF (7 mL), piperidine (1 mL), and ethanol (2 mL) and combined with $PdCl_2(PPh_3)_2$ (4.5 mg, 6.4 μmol, 2 mol %) and CuI (2.4 mg, 13 μmol, 4 mol %). Trimethyl((3-(trifluoromethyl)phenyl)ethynyl)-silane (194 mg, 0.801 mmol) and potassium hydroxide (157 mg, 2.80 mmol) were added, and the reaction was started with a heating gun. Salts started to precipitate immediately. The reaction mixture was stirred overnight at room temperature. The crude mixture was diluted with dichloromethane and washed three times with water, three times with brine, and once with aqueous ammonia hydroxide solution. The organic phase was dried with magnesium sulfate and evaporated under reduced pressure. The product was purified by crystallization from dichloromethane/hexanes yielding **8** (148 mg, 0.14 mmol, 45%) as an orange solid: mp 208−210 °C; ^{1}H NMR (500 MHz, THF-d_8) δ 0.86−0.91 (m, 6H), 1.28−1.34 (m, 8H), 1.43−1.51 (m, 4H), 1.81 (td, 4H, J = 7.5, 14.8 Hz), 3.92 (t, 4H, J = 7.1 Hz), 6.89 (dt, 2H, J = 1.0, 7.5 Hz), 6.94−6.97 (m, 4H), 7.09 (dd, 2H, J = 1.5, 7.6 Hz), 7.11−7.15 (m, 2H), 7.34 (d, 2H, J = 16.3 Hz), 7.40 (d, 2H, J = 1.9 Hz), 7.42 (dd, 2H, J = 1.9, 8.5 Hz), 7.59 (d, 2H, J = 16.3 Hz), 7.66 (t, 2H, J = 7.8 Hz), 7.74 (d, 2H, J = 7.9 Hz), 7.89 (d, 2H J = 7.7 Hz), 7.99 (s, 2 H), 8.02 (s, 2H); ^{13}C NMR (due to the very limited solubility of **8**, only an incomplete dataset could be obtained) δ 14.5, 23.7, 27.6, 28.0, 32.6, 48.3, 90.3, 94.8, 116.57, 116.60, 122.9, 123.4, 124.0, 125.4, 125.5, 126.3, 126.4, 127.1, 128.19, 128.23, 129.2, 129.9, 130.6, 131.3, 131.9, 132.1, 132.4, 132.9, 136.0, 138.7, 146.0, 146.5; IR (KBr) $\tilde{\nu}$ [cm^{-1}] 2958 (w), 2930 (w), 1632 (m),1602 (w), 1575 (w), 1496 (w), 1468 (m), 1443 (w), 1333 (w), 1247 (m), 1168 (m), 1129 (m), 800 (w), 746 (w), 694 (w); UV/vis (CH_2Cl_2) λ_{max} (ϵ) 250 nm (46000), 326 nm (81000), 340 nm (68000), 437 nm (54000); emission (CH_2Cl_2) λ_{max} (ϵ) 579 nm; MS (FAB$^+$) (*m*/*z* (%)) 1031 (21), 1030 (52), 1029 (M − H$^+$, 89), 1028 (M$^+$, 100), 1027 (15), 957 (12), 944 (14), 943 (19), 942 (17), 941 (40), 940 (58), 939 (39), 938 (40); HRMS calcd for $C_{64}H_{55}F_6N_2S_2$ 1029.3711, found 1029.3722.

3,3′-(1*E*,1′*E*)-2,2′-(2,5-Bis((3,5-bis(trifluoromethyl)phenyl)-ethynyl)-1,4-phenylene)bis(ethene-2,1-diyl)bis(10-hexyl-10*H*-phenothiazine) 9. An oven-dried Schlenk flask, cooled under nitrogen atmosphere, was charged with dry THF (2 mL), piperidine (1 mL), and ethanol (1 mL); potassium hydroxide (94.0 mg, 1.68 mmol), ((3,5-bis(trifluoromethyl)phenyl)ethynyl)trimethylsilane (149 mg, 0.480 mmol) and **4** (150 mg, 0.158 mmol) were added to the flask and were combined with $PdCl_2(PPh_3)_2$ (2.2 mg, 3.2 μmol, 2 mol %) and CuI (1.2 mg, 6.4 μmol, 4 mol %). The reaction mixture was heated to dissolve the diiodide completely. The reaction was stirred at room temperature overnight. The crude reaction mixture was diluted with dichloromethane and washed with brine and two times with 5% aqueous ammonia hydroxide solution, dried with magnesium sulfate, and concentrated under vacuum. The product was purified via crystallization from dichloromethane/toluene yielding **9** (38.0 mg, 0.03 mmol, 20%) as a sparingly soluble yellow powder: mp 240−242 °C; ^{1}H NMR (300 MHz, THF-d_8) δ 0.88−0.96 (m, 6H), 1.30−1.40 (m, 8H), 1.45−1.55 (m, 4H), 1.79−1.89 (m, 4H), 3.95 (t, 4H, J = 7.0 Hz), 6.89−7.03 (m, 6H), 7.10−7.20 (m, 4H), 7.37 (d, 2H, J = 16.2 Hz), 7.43−7.49 (m, 4H), 7.62 (d, 2H, J = 16.3 Hz), 8.11 (s, 2H), 8.13 (s, 2H), 8.32 (s, 4H); IR (KBr) $\tilde{\nu}$ [cm^{-1}] 2932 (w), 1630 (m), 1497 (w), 1486 (s), 1445 (w), 1373 (s), 1280 (s), 1248 (w), 1182 (m), 1137 (s), 894 (w), 746 (w), 698 (w), 684 (w); UV/vis (CH_2Cl_2) λ_{max} (ϵ) 252 nm (42000), 328 nm (70000), 414 nm (40000), 439 nm (43000); emission (CH_2Cl_2) λ_{max} (ϵ) 590 nm; MS (FAB$^+$) (*m*/*z* (%)) 1165 (M − H$^+$, 85), 1164 (M$^+$, 100), 1163 (15); HRMS calcd for $C_{66}H_{52}F_{12}N_2S_2$ 1164.3380, found 1164.3342; due to the insolubility of the cruciform, ^{13}C NMR could not be obtained.

Acknowledgment. We thank the Georgia Institute of Technology and the National Science Foundation (CHE 0548423) for generous financial support.

Supporting Information Available: A summary of the crystallographic data of **5** as cif file and details of the calculation for **5′**−**7′** as well as details for the optical spectroscopy of **5**−**9**. This material is available free of charge via the Internet at http://pubs.acs.org.

JO070922L